

# Infrared identification of the $\sigma$ -complex of Cl-C<sub>6</sub>H<sub>6</sub> in the reaction of chlorine atom and benzene in solid para-hydrogen

Mohammed Bahou, Henryk Witek, and Yuan-Pern Lee'

Citation: *J. Chem. Phys.* **138**, 074310 (2013); doi: 10.1063/1.4790860

View online: <http://dx.doi.org/10.1063/1.4790860>

View Table of Contents: <http://aip.scitation.org/toc/jcp/138/7>

Published by the [American Institute of Physics](#)

---

---



**PHYSICS  
TODAY**

*Physics Today* Buyer's Guide  
Search with a purpose.

# Infrared identification of the $\sigma$ -complex of Cl-C<sub>6</sub>H<sub>6</sub> in the reaction of chlorine atom and benzene in solid *para*-hydrogen

Mohammed Bahou,<sup>1</sup> Henryk Witek,<sup>1</sup> and Yuan-Pern Lee<sup>1,2,a)</sup>

<sup>1</sup>Department of Applied Chemistry and Institute of Molecular Science, National Chiao Tung University, 1001 Ta-Hsueh Road, Hsinchu 30010, Taiwan

<sup>2</sup>Institute of Atomic and Molecular Sciences, Academia Sinica, Taipei 10617, Taiwan

(Received 9 December 2012; accepted 25 January 2013; published online 19 February 2013)

The reaction of a chlorine atom with benzene (C<sub>6</sub>H<sub>6</sub>) is important in organic chemistry, especially in site-selective chlorination reactions, but its product has been a subject of debate for five decades. Previous experimental and theoretical studies provide no concrete conclusion on whether the product is a  $\pi$ - or  $\sigma$ -form of the Cl-C<sub>6</sub>H<sub>6</sub> complex. We took advantage of the diminished cage effect of *para*-hydrogen (*p*-H<sub>2</sub>) to produce Cl *in situ* to react with C<sub>6</sub>H<sub>6</sub> (or C<sub>6</sub>D<sub>6</sub>) upon photolysis of a Cl<sub>2</sub>/C<sub>6</sub>H<sub>6</sub> (or C<sub>6</sub>D<sub>6</sub>)/*p*-H<sub>2</sub> matrix at 3.2 K. The infrared spectrum, showing intense lines at 1430.5, 833.6, 719.8, 617.0, and 577.4 cm<sup>-1</sup>, and several weaker ones for Cl-C<sub>6</sub>H<sub>6</sub>, and the deuterium shifts of observed new lines unambiguously indicate that the product is a 6-chlorocyclohexadienyl radical, i.e., the  $\sigma$ -complex of Cl-C<sub>6</sub>H<sub>6</sub>. Observation of the  $\sigma$ -complex rather than the  $\pi$ -complex indicates that the  $\sigma$ -complex is more stable in solid *p*-H<sub>2</sub> at 3.2 K. The spectral information is crucial for further investigations of the Cl + C<sub>6</sub>H<sub>6</sub> reaction either in the gaseous or solution phase. © 2013 American Institute of Physics. [<http://dx.doi.org/10.1063/1.4790860>]

## I. INTRODUCTION

Rapid development of advanced experimental techniques and computational methods enables verification and detailed reinterpretation of many chemical reaction mechanisms, including identification and structural characterization of their transient intermediates<sup>1–3</sup> and explicit demonstration of realistic and not-so-fully-intuitive reaction pathways.<sup>4–7</sup> This development provides scientists a novel methodology for detailed investigations of fundamental organic reactions, which often seem to be a victim of oversimplified interpretations in organic chemistry textbooks. Chlorination reactions of aromatic compounds constitute such a class of organic reactions, mechanism of which is not yet fully understood. In the radical mechanism, it is believed that the initial step is the addition of a chlorine atom (Cl) to benzene (C<sub>6</sub>H<sub>6</sub>) to form a Cl-C<sub>6</sub>H<sub>6</sub> complex.<sup>8</sup> However, it has been highly contentious for more than 50 years whether the Cl-C<sub>6</sub>H<sub>6</sub> complex is a  $\pi$ - or  $\sigma$ -complex, i.e., whether the reaction between Cl and C<sub>6</sub>H<sub>6</sub> proceeds through a  $\pi$ - or  $\sigma$ -bonding.

In the 1950s, Russell and Brown postulated that Cl and C<sub>6</sub>H<sub>6</sub> form a hexahapto ( $\eta_6$ )  $\pi$ -complex (Figure 1(a)) to account for the enhanced selectivity of Cl with respect to the tertiary C–H bond of 2,3-dimethylbutane in organic photochlorination carried out in the presence of benzene.<sup>9–12</sup> A detailed study performed by Skell *et al.* under a broad range of experimental conditions suggested that the highly selective intermediate might be rather assigned to the 6-chlorocyclohexadienyl radical (the Cl-C<sub>6</sub>H<sub>6</sub>  $\sigma$ -complex, Figure 1(c)), whereas the low selective intermediates are best described as a mixture

of Cl atoms and the Cl-C<sub>6</sub>H<sub>6</sub>  $\pi$ -complex.<sup>13,14</sup> Ingold and co-workers employed laser flash photolysis to investigate the kinetics of these reactions in solutions and reported that the selectivity can be quantitatively described by a scheme which involves hydrogen abstraction by just two species, free Cl atoms and the  $\pi$ -complex.<sup>15–18</sup>

Theoretical characterization of the Cl-C<sub>6</sub>H<sub>6</sub> complexes proved to be a complex task. Tsao *et al.* employed various *ab initio* computational methods and density functional theory (DFT) to find that the  $\eta_6$   $\pi$ -complex and the  $\eta_2$   $\pi$ -complex (Figure 1(b)) have imaginary vibrational frequencies, hence, should be considered as transition states.<sup>19</sup> The stabilization energies of  $\sim 23$  and  $\sim 16$  kJ mol<sup>-1</sup> were predicted for the  $\eta_1$   $\pi$ -complex (Figure 1(d)) and the  $\sigma$ -complex, respectively, with the BH&HLYP/6-311++G\*\* method and the barrier height for the  $\eta_1$   $\pi$ -complex  $\rightarrow$   $\sigma$ -complex conversion was estimated as  $\sim 9$  kJ mol<sup>-1</sup>. The predicted values are within 5 kJ of those predicted with the CASPT2 method; the multi-reference character of  $\eta_1$   $\pi$ -complex makes the MP4(SDQ), CBS-QB&H, and CCSD(T) results unreliable.<sup>19</sup> The pronounced stability of the  $\eta_1$   $\pi$ -complex of Cl-C<sub>6</sub>H<sub>6</sub> was not confirmed by the study of Croft and Howard-Jones, who employed new density functionals designed particularly for non-covalent complexes and reported that the  $\sigma$ -complex is more stable than the  $\eta_1$   $\pi$ -complex, with a stabilization energy of 28–32 and 35–43 kJ mol<sup>-1</sup> predicted for the  $\eta_1$   $\pi$ -complex and the  $\sigma$ -complex, respectively, with the MPW1K method using various basis sets.<sup>20</sup> In view of these results, it is difficult to conclude unequivocally which of the Cl-C<sub>6</sub>H<sub>6</sub> complexes is the most stable.

The nature of the bonding between Cl and benzene in these two types of complexes is distinctly different despite of their similar energetics. Graphical explanation of the

<sup>a)</sup> Author to whom correspondence should be addressed. Electronic mail: yplee@mail.nctu.edu.tw.

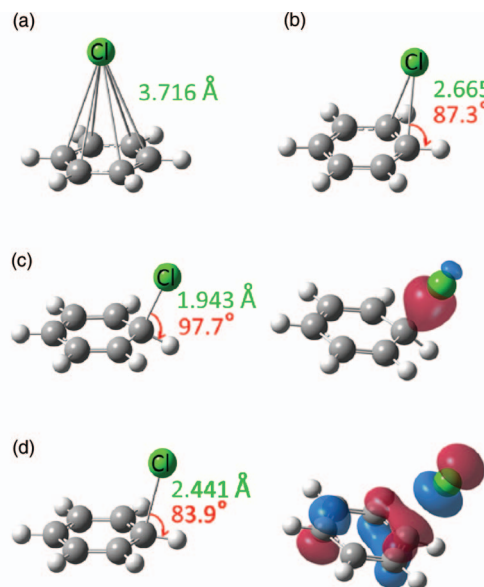


FIG. 1. Geometries of (a)  $\eta_6$   $\pi$ -complex, (b)  $\eta_2$   $\pi$ -complex, (c)  $\sigma$ -complex, and (d)  $\eta_1$   $\pi$ -complex predicted with the MPW1PW91/6-311++G(2d,2p) method. Bond distances are given in Å, and angles in degrees. For (c) and (d), a graphical representation of the bonding mechanism is also shown in the form of the bonding orbital.

bonding mechanism in the  $\sigma$ - and  $\pi$ -complexes of  $\text{Cl-C}_6\text{H}_6$ —represented in the form of bonding orbital between the Cl and  $\text{C}_6\text{H}_6$  moieties—is given in Figure 1(c) and 1(d). In the  $\pi$ -bonding scheme, the bonding is more delocalized and involves predominantly the bonding  $\pi$  orbitals associating with three carbon atoms of the benzene ring. In the  $\sigma$ -bonding scheme, Cl forms a  $\sigma$ -bond with one of the carbon atoms and consequently disrupts its aromaticity. As a result, the H atom on the chlorine-bonded carbon moves out of the molecular plane of benzene and the Cl—C distance is shorter. The difference in structure and bonding should result in distinct spectra of these complexes.

Spectral evidence for the existence of the  $\pi$ -complex rests on a broad transient absorption band near 490 nm and an intense broad band near 320 nm observed in pulse radiolysis of benzene in  $\text{CCl}_4$  solvent by Bühler.<sup>21,22</sup> They suggested that in the  $\pi$ -complex benzene acts as an electron donor and the chlorine atom as an electron acceptor; this feature resembles spectra of several other aromatic charge-transfer complexes. Bunce *et al.* also indicated that the 490 nm band, observed in their laser flash photolysis experiments, is unlikely due to a  $\sigma$ -compound, as usually  $\sigma$ -complexes absorb only weakly in the visible range.<sup>15</sup> In contrast, Bensen favors strongly the identification of this transient feature as belonging to the  $\sigma$ -complex.<sup>23</sup> The electron paramagnetic resonance (EPR) spectrum of the  $\text{Cl-C}_6\text{H}_6$  complex observed in irradiated frozen  $\text{Cl}_2/\text{C}_6\text{H}_6$  solid at 77 K indicates that this complex is most probably a distorted  $\sigma$ -complex.<sup>24</sup> Clearly, the available experimental (UV and EPR) and theoretical results do not permit for unambiguous assignment of the structure of the  $\text{Cl-C}_6\text{H}_6$  complex.

Infrared (IR) spectroscopy can provide more definitive information about molecular structures. Spectral characteri-

zation of distinct structural motifs for complexes of simple anions with arenes has been demonstrated clearly with IR spectroscopy.<sup>25</sup> Similarly, IR spectroscopy is expected to provide definitive structural information for this  $\text{Cl-C}_6\text{H}_6$  complex. If the  $\sigma$ -complex were formed, the characteristic C—H stretching mode below  $3000\text{ cm}^{-1}$  and the ClCH bending mode near  $1100\text{ cm}^{-1}$  for the newly formed ClCH moiety could be observed in the recorded IR spectrum, whereas if the  $\pi$ -complex were formed, the characteristic ring-stretching modes of the  $\text{C}_6\text{H}_6$  moiety near  $1600$  and  $950\text{ cm}^{-1}$  would be activated due to perturbation caused by the Cl atom.

Matrix isolation technique has proven to be an excellent method for investigating many unstable intermediates. Unfortunately, conventional matrix isolation techniques cannot be readily applied for studying reactions involving a single chlorine atom due to the fact that the *in situ* photolysis of the most common precursor,  $\text{Cl}_2$ , produces two Cl atoms, which cannot easily migrate out of the original matrix cage. Consequently, the reaction products typically contain two chlorine atoms.<sup>26</sup> An attractive alternative matrix host, which can be used to avoid this problem, is  $p\text{-H}_2$ . This quantum solid has emerged as a unique host for matrix isolation spectroscopy, with many excellent properties such as extremely narrow spectral width and a diminished matrix cage effect.<sup>27–29</sup> We have demonstrated that free radicals that are difficult to be produced using conventional inert-gas matrices can be readily produced in a  $p\text{-H}_2$  matrix via photolysis *in situ*<sup>30</sup> or photo-induced bimolecular reactions.<sup>31,32</sup> Here we took advantage of the diminished cage effect of  $p\text{-H}_2$  to produce chlorine atoms from *in situ* photolysis of  $\text{Cl}_2$  in a  $\text{Cl}_2/\text{C}_6\text{H}_6/p\text{-H}_2$  matrix at 3.2 K; subsequent reaction between Cl and  $\text{C}_6\text{H}_6$  produces the  $\text{Cl-C}_6\text{H}_6$  complex. As we demonstrate below, the observed IR spectra and deuterium isotopic shifts clearly indicate that the  $\text{Cl-C}_6\text{H}_6$  produced in these experiments is a  $\sigma$ -complex.

## II. EXPERIMENTS

The experimental setup has been described previously.<sup>26,31</sup> In these experiments, a gold-plated copper plate served both as a cold substrate for the matrix sample and as a mirror to reflect the incident IR beam to the detector. The copper plate was maintained at 3.2 K with a closed-cycle helium refrigerator (Janis, SHI-415). Typically, gaseous mixtures of  $\text{C}_6\text{H}_6/p\text{-H}_2$  (1/750, 0.02 mol) and  $\text{Cl}_2/p\text{-H}_2$  (1/750, 0.02 mol) were co-deposited over a period of 5 h. The 365 nm light from a light-emitting diode (375 mW) was employed to dissociate  $\text{Cl}_2$  to produce Cl atoms. IR absorption spectra were recorded with a Fourier-transform infrared (FTIR) spectrometer (Bomem, DA8) equipped with a KBr beamsplitter and a Hg/Cd/Te detector (cooled to 77 K) to cover the spectral range  $500\text{--}4000\text{ cm}^{-1}$ . Typically, 400 scans at a resolution of  $0.25\text{ cm}^{-1}$  were recorded at each stage of the experiment. It has been previously reported that infrared excitation of the solid  $p\text{-H}_2$  bands ( $4000\text{--}5000\text{ cm}^{-1}$ ) can induce Cl atoms to react with  $p\text{-H}_2$  to form  $\text{HCl}$ ,<sup>33</sup> and therefore, when Cl atoms were present in the  $p\text{-H}_2$  matrix, a  $2.4\text{ }\mu\text{m}$  infrared cutoff filter (Andover Corp.) was used when recording the infrared spectra.

Flow rates of  $\text{C}_6\text{H}_6/p\text{-H}_2$  and  $\text{Cl}_2/p\text{-H}_2$  are typically 0.08–0.11 and 0.055–0.12  $\text{mmol h}^{-1}$ , respectively.  $\text{C}_6\text{H}_6$  (99.5%, Fluka),  $\text{C}_6\text{D}_6$  (listed isotopic purity 99.5%, Cambridge Isotope Laboratories, Inc), and  $\text{Cl}_2$  (99.9%, Air Products and Chemicals) were used without further purification.  $\text{H}_2$  (99.9999%, Scott Specialty Gases) was used after passage through a trap at 77 K before conversion to  $p\text{-H}_2$ . The  $p\text{-H}_2$  converter comprised a copper cell filled with hydrous iron (III) oxide catalyst (Aldrich) and cooled with a closed-cycle refrigerator (Advanced Research Systems, DE204AF). The efficiency of conversion is controlled by the temperature of the catalyst; at 11.5 K, the concentration of  $o\text{-H}_2$  is <10 ppm.

### III. RESULTS AND DISCUSSION

#### A. Cl + $\text{C}_6\text{H}_6$ reaction

The partial IR spectrum of a deposited sample of  $\text{Cl}_2/\text{C}_6\text{H}_6/p\text{-H}_2$  (1/1/1500) at 3.2 K (Figure 2(a)) exhibits absorption lines of  $\text{C}_6\text{H}_6$  and also complexes of  $\text{C}_6\text{H}_6\text{-Cl}_2$  (indicated with \*).  $\text{C}_6\text{H}_6\text{-Cl}_2$  has been observed in solid  $\text{N}_2$ .<sup>34</sup> Spectra covering a wider spectral range and a comparison of the experimental and theoretical frequencies and relative intensities of  $\text{C}_6\text{H}_6\text{-Cl}_2$  are available in the supplementary material.<sup>35</sup> Upon irradiation with light at 365 nm for 5 h, the intensities of IR lines due to  $\text{C}_6\text{H}_6$  and  $\text{C}_6\text{H}_6\text{-Cl}_2$  complexes decreased slightly, and several new features appeared. A difference spectrum obtained by subtracting the spectrum of the deposited matrix from the spectrum recorded after irradiation at 365 nm is presented in Figure 2(b); lines pointing upwards indicate production and those pointing downwards indicate destruction. Annealing of the irradiated matrix at 5 K for 2 min enhanced some of these new features significantly and further diminished the absorption lines of  $\text{C}_6\text{H}_6$ , as shown in the difference spectrum in Figure 2(c). Secondary photolysis

of this matrix with light in the 455–700 nm region diminished these features further and enabled us to identify clearly lines associated with a single species, as indicated with arrows in Figure 2(d). Intense features at 577.4, 617.0, 719.8, 833.6, and 1430.5  $\text{cm}^{-1}$  and weaker ones at 876.8, 956.0, 1008.0, 1026.4, 1179.0, 1406.5, and 1509.4  $\text{cm}^{-1}$  are clearly identified. Common origin of these features is further confirmed by comparison of spectra recorded at various stages of the experiment and in several different experiments.

The identification of the molecular species responsible for the observed additional IR signals is not a difficult puzzle. Upon irradiation of  $\text{Cl}_2$  at 365 nm, Cl atoms were produced and subsequently reacted with  $\text{C}_6\text{H}_6$ , as indicated by the decreased absorption of  $\text{C}_6\text{H}_6$  and  $\text{C}_6\text{H}_6\text{-Cl}_2$ . The new features thus produced are expected to originate from the products of the  $\text{Cl} + \text{C}_6\text{H}_6$  reaction. Further evidence comes from the enhancement of these features after annealing, which can be explained by higher mobility of the Cl atoms at 5 K and lack of photolysis. At low temperatures and without irradiation, the hydrogen abstraction cannot occur because of a large barrier associated with this reaction channel. The only viable reaction channels lead hence to the formation of the  $\text{Cl-C}_6\text{H}_6$  complexes. The secondary photolysis in the 455–700 nm region might dissociate some  $\sigma$ -complex of  $\text{Cl-C}_6\text{H}_6$ , which absorbs in the visible region.<sup>14</sup>

The IR spectra of each specific  $\text{Cl-C}_6\text{H}_6$  complex simulated with various theoretical models yield similar spectral patterns; the largest discrepancies concern only some small shifts in the positions of the bands. We present here only calculation results from the MPW1PW91/6-311++G(2d,2p) method; this method was chosen because it was designed particularly for non-covalent complexes.<sup>20</sup> A comparison of the new spectral features observed in the experiment for the  $\text{Cl-C}_6\text{H}_6$  complex (Figure 3(a)) with the stick IR spectra

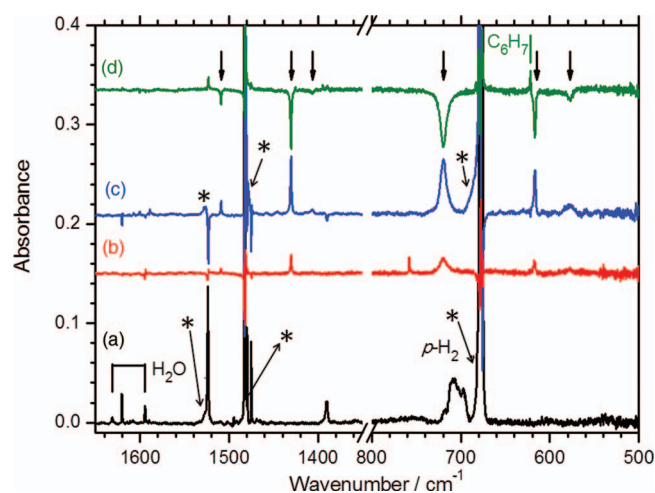


FIG. 2. (a) IR absorption spectra of a  $\text{Cl}_2/\text{C}_6\text{H}_6/p\text{-H}_2$  (1/1/1500) matrix sample after deposition at 3.2 K for 5 h. (b) Difference spectra after irradiation of the matrix with a LED at 365 nm for 1 h. (c) After annealing the sample at 5 K for 2 min. (d) After secondary photolysis at 3.2 K in the range 455–700 nm from a Hg lamp for 1 h. Lines of the  $\text{C}_6\text{H}_6\text{-Cl}_2$  complex are indicated with asterisks (\*). New lines attributable to  $\text{Cl-C}_6\text{H}_6$  are indicated with arrows.

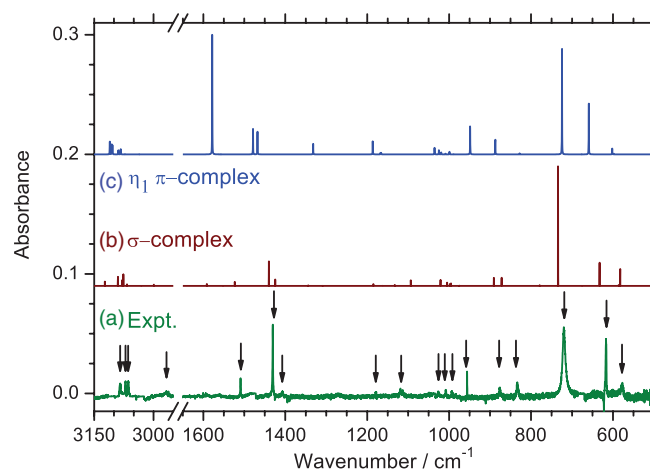


FIG. 3. (a) Difference IR absorption spectra of a  $\text{Cl}_2/\text{C}_6\text{H}_6/p\text{-H}_2$  (1/1/1500) matrix sample after secondary photolysis in the range 455–700 nm from a Hg lamp at 3.2 K for 1 h; the matrix was deposited at 3.2 K for 5 h, followed by irradiation with a LED at 365 nm for 1 h and annealing the sample at 5 K for 2 min. Lines of  $\text{C}_6\text{H}_6$  are removed for clarity. IR spectra of the  $\sigma$ -complex (b) and the  $\eta_1$   $\pi$ -complex (c) of  $\text{Cl-C}_6\text{H}_6$  simulated according to the anharmonic vibrational frequencies and IR intensities predicted with the MPW1PW91/6-311++G(2d,2p) method. New lines attributable to  $\text{Cl-C}_6\text{H}_6$  are indicated with arrows.



of the  $\sigma$ -complex (Figure 3(b)) and the  $\eta_1$   $\pi$ -complex (Figure 3(c)), simulated according to anharmonic vibrational frequencies and IR intensities computed with the MPW1PW91/6-311++G(2d,2p) method, suggests that the best agreement in terms of relative intensities and positions is obtained for the predicted spectrum of the  $\sigma$ -complex. The  $\eta_1$   $\pi$ -complex is predicted to have intense lines at 659 (44), 725 (88), 887 (13), 1186 (12), 1479 (22), 1468 (21), and 1578 (100)  $\text{cm}^{-1}$ , whereas the  $\sigma$ -complex is predicted to have intense lines at 582 (13), 633 (22), 734 (100), 872 (7), and 1440 (19)  $\text{cm}^{-1}$ ; numbers in parentheses give relative IR intensities. Intense lines at 577.4 (19), 617.0 (26), 719.8 (100), 833.6 (11), and 1430.5 (25)  $\text{cm}^{-1}$  observed in this work are consistent with those predicted for the  $\sigma$ -complex. A list of wavenumbers and relative intensities for the observed lines and their comparison with calculations is given in Table I;

TABLE I. Comparison of experimentally observed line positions ( $\text{cm}^{-1}$ ) and intensities with the computed MPW1PW91/6-311++G(2d,2p) anharmonic vibrational wavenumbers ( $\text{cm}^{-1}$ ) and IR intensities of the  $\sigma$ - and  $\pi$ -complexes of Cl-C<sub>6</sub>H<sub>6</sub>.

Mode <sup>a</sup>	Sym.	$\eta_1$ $\pi$ -complex	$\sigma$ -complex	Experiment
$\nu_1$	$a'$	3104 (7) <sup>b</sup>	3123 (3) <sup>b</sup>	
$\nu_2$	$a'$	3089 (3)	3090 (7)	3070.9 (7.6) <sup>c</sup>
$\nu_3$	$a'$	3111 (10)	3067 (1)	3054.3 (0.5)
$\nu_4$	$a'$	3072 (0)	2999 (1)	2967.2 (2.3)
$\nu_5$	$a'$	1578 (100)	1591 (1)	
$\nu_6$	$a'$	1468 (21)	1440 (19)	1430.5 (25)
$\nu_7$	$a'$	1186 (12)	1185 (2)	1179.0 (0.2)
$\nu_8$	$a'$	1025 (4)	1094 (4)	1112.5 (1.4)
$\nu_9$	$a'$	1019 (2)	1005 (3)	1008.0 (2.9)
$\nu_{10}$	$a'$	1009 (1)	998 (2)	993.5 (3.7)
$\nu_{11}$	$a'$	999 (2)	996 (2)	983.0 (1.4)
$\nu_{12}$	$a'$	949 (27)	891 (6)	876.8 (4.8)
$\nu_{13}$	$a'$	887 (13)	872 (7)	833.6 (11)
$\nu_{14}$	$a'$	725 (88)	734 (100)	719.8 (100)
$\nu_{15}$	$a'$	659 (44)	633 (22)	617.0 (26)
$\nu_{16}$	$a'$	602 (5)	582 (13)	577.4 (19)
$\nu_{17}$	$a'$	376 (4)	391 (19)	
$\nu_{18}$	$a'$	94 (1)	224 (72)	
$\nu_{19}$	$a'$	92 (4)	91 (0)	
$\nu_{20}$	$a''$	3106 (9)	3076 (9)	3083.9 (10)
$\nu_{21}$	$a''$	3083 (4)	3079 (5)	3063.4 (7.9)
$\nu_{22}$	$a''$	1562 (0)	1523 (3)	1509.4 (4.0)
$\nu_{23}$	$a''$	1479 (22)	1425 (6)	1406.5 (2.9)
$\nu_{24}$	$a''$	1354 (0)	1344 (0)	
$\nu_{25}$	$a''$	1332 (8)	1309 (0)	
$\nu_{26}$	$a''$	1168 (1)	1162 (0)	
$\nu_{27}$	$a''$	1166 (1)	1133 (1)	1118.5 (2.5)
$\nu_{28}$	$a''$	1036 (5)	1021 (5)	1026.4 (1.2)
$\nu_{29}$	$a''$	989 (0)	975 (0)	956.0 (3.0)
$\nu_{30}$	$a''$	828 (1)	779 (1)	
$\nu_{31}$	$a''$	598 (0)	586 (1)	
$\nu_{32}$	$a''$	389 (0)	404 (0)	
$\nu_{33}$	$a''$	101 (1)	202 (1)	

<sup>a</sup>Mode numbers follow the order of the wavenumbers predicted for the  $\sigma$ -complex of Cl-C<sub>6</sub>H<sub>6</sub>.

<sup>b</sup>Relative IR intensities normalized to the most intense line. IR intensities for the most intense lines of  $\eta_1$   $\pi$ -complex and  $\sigma$ -complex are 71.2 and 100.3  $\text{km mol}^{-1}$ , respectively.

<sup>c</sup>Integrated IR intensities relative to  $\nu_{14}$  are listed in parentheses.

nearly all lines of the  $\sigma$ -complex with computed IR intensity greater than 2  $\text{km mol}^{-1}$  are observed in experiment. Although weak, the C–H stretching and the ClCH bending modes of the C(Cl)H moiety were observed at 2967.2 and 1112.5  $\text{cm}^{-1}$ , respectively, similar to the predicted values of 2999 and 1094  $\text{cm}^{-1}$ . In contrast, the intense ring-stretching mode predicted near 1578  $\text{cm}^{-1}$  for the  $\pi$ -complex was unobserved.

We observed larger bandwidths for lines at 577.4, 617.0, 719.8, 833.6, and 876.8  $\text{cm}^{-1}$  that are associated with vibrational modes involving significant change of the Cl–C distance. The observed broadening might be because the increase in the Cl–C distance upon vibrational excitation leads to dissociation of the complex or because of the flat potential energy surface along the C–Cl stretching coordinate that allows a variety of structures with slightly different vibrational frequencies for these modes. Considering the stabilization energy of 19–43  $\text{kJ mol}^{-1}$  predicted for the Cl–C<sub>6</sub>H<sub>6</sub> complex and the low temperature, the latter explanation is more likely.

Previous reports suggested that in the  $\pi$ -complex benzene acts as an electron donor and the chlorine atom as an electron acceptor. A transient broad absorption band near 490 nm observed in pulse radiolysis of benzene in CCl<sub>4</sub> solvent by Bühler resembles spectra of several other aromatic charge-transfer complexes.<sup>21,22</sup> Our calculations do not confirm the assumed sharp dichotomy between the charge-transfer characters of the  $\sigma$ - and  $\pi$ -complexes; electrostatic potentials computed for both complexes look very much alike, as shown in the supplementary material.<sup>35</sup>

Theoretical calculations using the BH&HLYP/6-311++G\*\*(5D) time-dependent density functional theory (TD-DFT) method predicted one intense band ( $f = 0.208$ ) near 456 nm and one medium band ( $f = 0.050$ ) near 335 nm for the  $\pi$ -complex, and one weak band

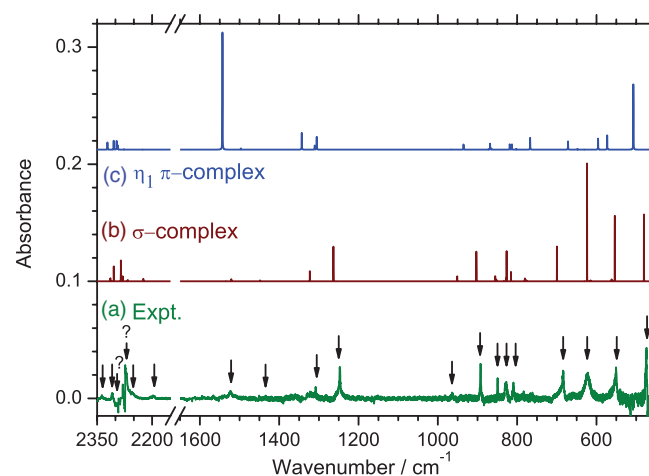


FIG. 4. (a) Inverted difference IR absorption spectra of a Cl<sub>2</sub>/C<sub>6</sub>D<sub>6</sub>/*p*-H<sub>2</sub> (1/1/2000) matrix sample after secondary photolysis in the range 455–700 nm from a Hg lamp at 3.2 K for 1 h; the matrix was deposited at 3.2 K for 5 h, followed by irradiation with a LED at 365 nm for 1 h and annealing the sample at 5 K for 2 min. (b) Lines of C<sub>6</sub>H<sub>6</sub> are removed for clarity. IR spectra of the  $\sigma$ -complex. (c) The  $\eta_1$   $\pi$ -complex of Cl-C<sub>6</sub>D<sub>6</sub> simulated according to the anharmonic vibrational frequencies and IR intensities predicted with the MPW1PW91/6-311++G(2d,2p) method. New lines attributable to Cl-C<sub>6</sub>H<sub>6</sub> are indicated with arrows.

( $f = 0.003$ ) near 416 nm and a medium band ( $f = 0.016$ ) near 296 nm for the  $\sigma$ -complex. Our calculations using the TDDFT/MPW1PW91/6-311++G(2d,2p) method yield bands near 404 nm ( $f = 0.118$ ) and 307 nm ( $f = 0.058$ ) for the  $\pi$ -complex and 478 nm ( $f = 0.003$ ) and 305 nm ( $f = 0.047$ ) for the  $\sigma$ -complex. Hence, the  $\sigma$ -complex is likely photolyzed with light in the region 455–700 nm so that we observed the decrease in intensity for lines of the  $\sigma$ -complex.

## B. Cl + C<sub>6</sub>D<sub>6</sub> reaction

A similar experiment was performed with Cl<sub>2</sub>/C<sub>6</sub>D<sub>6</sub>/*p*-H<sub>2</sub> (1/1/1200). We show in Figure 4(a) the inverted difference spectrum of the matrix after 1 h of secondary irradiation with the 455–700 nm light; the matrix was initially irradiated with light at 365 nm for 1 h, followed by annealing at 5 K for 2 min

TABLE II. Comparison of experimentally observed line positions (cm<sup>-1</sup>) and intensities with the computed MPW1PW91/6-311++g(2d,2p) anharmonic vibrational wavenumbers (cm<sup>-1</sup>) and IR intensities of the  $\sigma$ - and  $\pi$ -complexes of Cl-C<sub>6</sub>D<sub>6</sub>.

Mode <sup>a</sup>	Sym.	$\eta_1$ $\pi$ -complex	$\sigma$ -complex	Experiment
$\nu_1$	a'	2322 (5) <sup>b</sup>	2314 (3) <sup>b</sup>	2336.0 (3.8) <sup>c</sup>
$\nu_2$	a'	2294 (3)	2305 (14)	2308.6 (8.4)
$\nu_3$	a'	2297 (8)	2267 (2)	2255.3 (1.8)?
$\nu_4$	a'	2276 (0)	2224 (2)	2197.4 (9.3)
$\nu_5$	a'	1543 (100)	1521 (2)	1523.3 (8.0)
$\nu_6$	a'	1305 (11)	1263 (29)	1247.1 (46)
$\nu_7$	a'	868 (4)	855 (5)	849.4 (5.5)
$\nu_8$	a'	813 (4)	827 (27)	828.0 (25)
$\nu_9$	a'	966 (0)	903 (25)	892.3 (32)
$\nu_{10}$	a'	935 (4)	951 (5)	963.0 (2.5)
$\nu_{11}$	a'	872 (0)	828 (3)	
$\nu_{12}$	a'	767 (8)	777 (2)	761.7 (1.3)
$\nu_{13}$	a'	672 (6)	700 (29)	683.6 (34)
$\nu_{14}$	a'	507 (50)	624 (100)	622.6 (100)
$\nu_{15}$	a'	596 (9)	480 (56)	474.1 (59)
$\nu_{16}$	a'	573 (10)	554 (53)	550.5 (51)
$\nu_{17}$	a'	333 (4)	341 (49)	
$\nu_{18}$	a'	93 (1)	219 (159)	
$\nu_{19}$	a'	88 (3)	84 (2)	
$\nu_{20}$	a''	2305 (7)	2285 (17)	2293.2 (1.7)
$\nu_{21}$	a''	2294 (1)	2280 (5)	2269.3 (1.0)
$\nu_{22}$	a''	1497 (1)	1448 (0)	1433.8 (0.8)
$\nu_{23}$	a''	1343 (15)	1323 (8)	1308.4 (4.6)
$\nu_{24}$	a''	1060 (0)	1055 (0)	
$\nu_{25}$	a''	1310 (3)	1257 (0)	
$\nu_{26}$	a''	865 (1)	833 (0)	
$\nu_{27}$	a''	834 (0)	853 (2)	
$\nu_{28}$	a''	819 (4)	828 (8)	809.1 (19)
$\nu_{29}$	a''	802 (1)	781 (2)	
$\nu_{30}$	a''	648 (1)	615 (2)	
$\nu_{31}$	a''	571 (0)	562 (2)	
$\nu_{32}$	a''	338 (0)	351 (0)	
$\nu_{33}$	a''	89 (1)	187 (2)	

<sup>a</sup>Mode numbers follow the order of the wavenumbers predicted for the  $\sigma$ -complex of Cl-C<sub>6</sub>D<sub>6</sub>.

<sup>b</sup>Relative IR intensities normalized to the most intense line in our detection range. IR intensities for these lines of  $\eta_1$   $\pi$ -complex and  $\sigma$ -complex are 79.5 and 40.6 km mol<sup>-1</sup>, respectively.

<sup>c</sup>Integrated IR intensities relative to  $\nu_{14}$  are listed in parentheses.

before this step. New features at 474.1, 550.5, 622.6, 683.6, 1247.1, 1308.4, 1433.8, and 1523.3 cm<sup>-1</sup> are indicated with arrows. The spectrum is compared with the IR spectra of Cl-C<sub>6</sub>D<sub>6</sub> for the  $\sigma$ -complex (Figure 4(b)) and the  $\eta_1$   $\pi$ -complex (Figure 4(c)) simulated according to anharmonic vibrational frequencies and IR intensities predicted with the MPW1PW91/6-311++G(2d,2p) method. A comparison of the experimental and theoretical frequencies and relative intensities is given in Table II. The excellent agreement between the experimental and theoretical spectra for the  $\sigma$ -complex further supports our assignments.

## IV. CONCLUSION

In summary, the work presented in this report clearly demonstrates that the product of the reaction of the Cl atom with the C<sub>6</sub>H<sub>6</sub> molecule in solid *p*-H<sub>2</sub> is the  $\sigma$ -complex (6-chlorocyclohexadienyl radical) rather than the  $\pi$ -complex. This observation indicates that the  $\sigma$ -complex isolated in solid *p*-H<sub>2</sub> at 3.2 K is likely lower in energy than the  $\pi$ -complex. Although we expect that the matrix effect in solid *p*-H<sub>2</sub> is small, it is unclear if our conclusion on the relative stability of the complexes can be extended to the reaction of Cl + C<sub>6</sub>H<sub>6</sub> in solutions. Nevertheless, the IR absorption spectrum reported in this work provides definitive structural characterization of the Cl-C<sub>6</sub>H<sub>6</sub>  $\sigma$ -complex as the 6-chlorocyclohexadienyl radical, and is crucial for further investigations of the Cl + C<sub>6</sub>H<sub>6</sub> reaction either in the gaseous or solution phase.

## ACKNOWLEDGMENTS

National Science Council of Taiwan (Grant Nos. NSC100-2745-M009-001-ASP and NSC99-2113-M-009-011-MY3) and the Ministry of Education, Taiwan ("Aim for the Top University Plan" of National Chiao Tung University) supported this work. The National Center for High-Performance Computing provided computer time.

<sup>1</sup>K. Suma, Y. Sumiyoshi, and Y. Endo, *Science* **308**, 1885 (2005).

<sup>2</sup>O. Asvany, P. Kumar, P. B. Redlich, I. Hegemann, S. Schlemmer, and D. Marx, *Science* **309**, 1219 (2005).

<sup>3</sup>S. Narra, S.-W. Chang, H. A. Witek, and S. Shigeto, *Chem.-Eur. J.* **18**, 2543 (2012).

<sup>4</sup>A. K. Mollner, S. Valluvadasan, L. Feng, M. K. Sprague, M. Okumura, D. B. Milligan, W. J. Bloss, S. P. Sander, P. T. Martien, R. A. Harley, A. B. McCoy, and W. P. L. Carter, *Science* **330**, 646 (2010).

<sup>5</sup>P. R. Schreiner, H. P. Reisenauer, D. Ley, D. Gerbig, C.-H. Wu, and W. D. Allen, *Science* **332**, 1300 (2011).

<sup>6</sup>M. P. Grubb, M. L. Warter, H. Xiao, S. Maeda, K. Morokuma, and S. W. North, *Science* **335**, 1075 (2012).

<sup>7</sup>D. Townsend, S. A. Lahankar, S. K. Lee, S. D. Chambreau, A. G. Suits, X. Zhang, J. Rheinecker, L. B. Harding, and J. M. Bowman, *Science* **306**, 1158 (2004).

<sup>8</sup>J. M. Tanko and N. K. Suleman, in *Energetics of Organic Free Radicals*, edited by J. A. M. Simões, J. F. Liebman, and A. Greenberg (Chapman and Hall, New York, 1996), Chap. VIII.

<sup>9</sup>G. A. Russell and H. C. Brown, *J. Am. Chem. Soc.* **77**, 4031 (1955).

<sup>10</sup>G. A. Russell, *J. Am. Chem. Soc.* **79**, 2977 (1957).

<sup>11</sup>G. A. Russell, *J. Am. Chem. Soc.* **80**, 4987 (1958).

<sup>12</sup>G. A. Russell, *J. Am. Chem. Soc.* **80**, 4997 (1958).

<sup>13</sup>P. S. Skell, H. N. Baxter III, and C. K. Taylor, *J. Am. Chem. Soc.* **105**, 120 (1983).

<sup>14</sup>P. S. Skell, H. N. Baxter III, J. M. Tanko, and V. Chebolu, *J. Am. Chem. Soc.* **108**, 6300 (1986).

- <sup>15</sup>N. J. Bunce, K. U. Ingold, J. P. Landers, J. Lusztyk, and J. C. Scaiano, *J. Am. Chem. Soc.* **107**, 5464 (1985).
- <sup>16</sup>K. U. Ingold, J. Lusztyk, and K. D. Raner, *Acc. Chem. Res.* **23**, 219 (1990).
- <sup>17</sup>K. D. Rander, J. Lusztyk, and K. U. Ingold, *J. Phys. Chem.* **93**, 564 (1989).
- <sup>18</sup>K. D. Rander, J. Lusztyk, and K. U. Ingold, *J. Am. Chem. Soc.* **110**, 3519 (1988).
- <sup>19</sup>M.-L. Tsao, C. M. Hadad, and M. S. Platz, *J. Am. Chem. Soc.* **125**, 8390 (2003).
- <sup>20</sup>A. K. Croft and H. M. Howard-Jones, *Phys. Chem. Chem. Phys.* **9**, 5649 (2007).
- <sup>21</sup>R. E. Bühler and M. Ebert, *Nature (London)* **214**, 1220 (1967).
- <sup>22</sup>R. E. Bühler, *Helv. Chim. Acta* **51**, 1558 (1968).
- <sup>23</sup>S. W. Benson, *J. Am. Chem. Soc.* **115**, 6969 (1993).
- <sup>24</sup>G. B. Sergeev, A. V. Pukhovskii, and V. V. Smirov, *Russ. J. Phys. Chem.* **57**, 589 (1983).
- <sup>25</sup>B. Chiavarino, M. E. Crestoni, S. Fornarini, F. Lanucara, J. Lemaire, P. Maître, and D. Scuderi, *Chem.-Eur. J.* **15**, 8185 (2009).
- <sup>26</sup>C.-W. Huang, Y.-C. Lee, and Y.-P. Lee, *J. Chem. Phys.* **132**, 164303 (2010).
- <sup>27</sup>T. Oka, *Annu. Rev. Phys. Chem.* **44**, 299 (1993).
- <sup>28</sup>T. Momose and T. Shida, *Bull. Chem. Soc. Jpn.* **71**, 1 (1998).
- <sup>29</sup>K. Yoshioka and D. T. Anderson, *J. Chem. Phys.* **119**, 4731 (2003).
- <sup>30</sup>M. Bahou and Y.-P. Lee, *J. Chem. Phys.* **133**, 164316 (2010).
- <sup>31</sup>J. Amicangelo and Y.-P. Lee, *J. Phys. Chem. Lett.* **1**, 2956 (2010).
- <sup>32</sup>Y.-F. Lee and Y.-P. Lee, *J. Chem. Phys.* **134**, 124314 (2011).
- <sup>33</sup>P. L. Raston and D. T. Anderson, *Phys. Chem. Chem. Phys.* **8**, 3124 (2006).
- <sup>34</sup>L. Fredin and B. Nelander, *Mol. Phys.* **27**, 885 (1974).
- <sup>35</sup>See supplementary material at <http://dx.doi.org/10.1063/1.4790860> for schematic representation of the electrostatic potential of the Cl-C<sub>6</sub>H<sub>6</sub> complexes, experimental spectra covering a wider spectral range, and a comparison of the experimental and theoretical frequencies and relative intensities of C<sub>6</sub>H<sub>6</sub> and C<sub>6</sub>H<sub>6</sub>-Cl<sub>2</sub>.